

Synchronization of networks with variable local properties

Jesús Gómez-Gardeñes^{1,2} and Yamir Moreno¹

¹*Institute for Biocomputation and Physics of Complex Systems (BIFI), University of Zaragoza, Zaragoza 50009, Spain*

²*Departamento de Física de la Materia Condensada, University of Zaragoza, Zaragoza E-50009, Spain*

(Dated: January 7, 2022)

We study the synchronization transition of Kuramoto oscillators in scale-free networks that are characterized by tunable local properties. Specifically, we perform a detailed finite size scaling analysis and inspect how the critical properties of the dynamics change when the clustering coefficient and the average shortest path length are varied. The results show that the onset of synchronization does depend on these properties, though the dependence is smooth. On the contrary, the appearance of complete synchronization is radically affected by the structure of the networks. Our study highlights the need of exploring the whole phase diagram and not only the stability of the fully synchronized state, where most studies have been done up to now.

PACS numbers: 05.45.Xt, 89.75.Fb

INTRODUCTION

Emergent collective phenomena have been studied since long time ago. These phenomena arise in many fields of science, ranging from natural to social and artificial systems. They are characterized, among other features, by the collective behavior of many interacting units that show a pattern hard to predict from the individual behavior of the system constituents. Several seminal models of statistical physics and non-linear dynamics have been scrutinized as paradigms of self-organization, emergence and cooperation between the units forming the system. In particular, synchronization phenomena constitute one of the most striking examples because of the many systems showing synchronization patterns in their behavior [1, 2, 3].

One of the most celebrated synchronization models is due to Kuramoto [4, 5], who analyzed a model of phase oscillators coupled through a function (sine) of their phase differences. This model owes most of its success to the plenty of analytical insights that one can get through the mean-field approximation originally proposed by Kuramoto. In this approach (KM), the nodes of an all to all, i.e. globally, coupled network, are considered to be oscillators with an intrinsic frequency and their phases evolve in time in such a way that if the coupling between them is larger than a critical threshold, the whole system gets locked in phase and attains complete synchronization.

However, it has been recently discovered that real systems do not show a homogeneous pattern of interconnections among their parts. That is, the underlying structure is not compatible with the original assumption of the KM. It is not even well described by random patterns of interconnections in the vast majority of systems. Therefore, the mean-field approach requires of several constraints that are not usually fulfilled in real systems. Natural, social and technological systems show complex patterns of connectivity that characterize seemingly diverse social [6], biological [7, 8] and technological systems [9, 10]. They exhibit common features that can be captured using the tools of graph theory or in more recent terms, network modeling [11, 12, 13].

It turns out that many real networks are well described by the so-called scale-free (SF) networks. Their main feature is that the probability that a given node has k connections to other nodes follows a power-law $P_k \sim k^{-\gamma}$, with $2 \leq \gamma \leq 3$ in most cases [11, 13]. The study of processes taking place on top of these networks has led to reconsider classical results obtained for regular lattices or random graphs due to the radical changes of the system's dynamics when the heterogeneity of complex networks can not be neglected [11, 12, 13, 14, 15, 16, 17].

It is then natural to investigate how synchronization phenomena in real systems are affected by the complex topological patterns of interaction. This is not an easy task, as one has to deal with two sources of complexity, the nonlinear character of the dynamics and highly non trivial complex structures. In recent years, scientists have addressed the problem of synchronization capitalizing on the Master Stability Function (MSF) formalism [18] which allows to study the stability of the *fully synchronized state* [19, 20, 21, 22, 23, 24]. While the MSF approach is useful to get a first insight into what is going on in the system as far as the stability of the synchronized state is concerned, it tells nothing about how synchronization is attained and whether or not the system under study exhibits a critical point similar to the original KM. To this end, one must rely on numerical calculations and explore the *entire phase diagram*. Surprisingly, there are only a few works that have dealt with the study of the whole synchronization dynamics in specific scenarios [25, 26, 27, 28, 29, 30] as compared with those where the MSF is used, given that the onset of synchronization is reached in its behavioral repertoire than the state of complete synchronization.

In this paper, we take a further step in the detailed characterization of the phase diagram and specifically, in the description of the dynamical behavior at the onset of synchronization in SF networks. By performing a standard finite size scaling analysis, we show that the local topology affects the critical properties of the dynamics, though it is less pronounced than what one may expect a priori. We capitalize on a network model that keeps the power-law exponent fixed while varying the clustering coefficient and the average path length. In what

follows, we describe the topological and dynamical model and discuss the results from a global perspective. Finally, in the last section, we state our conclusions.

NETWORK MODEL AND DYNAMICS

We implement a network model in which the graph is grown at each time step by linking preferentially new nodes to already existing nodes in the same way as in the Barabasi and Albert (BA) model [31]. The only difference is that the nodes are assumed to have a fitness that characterizes their affinities [32]. In this way, by tuning a single parameter μ , one can go from the BA limit down to a network in which several network properties vary as a function of μ . On the other hand, as the linking mechanism is still the BA preferential attachment rule, the exponent γ of the power-law degree distribution is the same (i.e., $\gamma = 3$) regardless of the value of μ . Roughly speaking, the model mimics the situation in which new nodes are attached to an existing core or network but without having knowledge of the whole topology.

The recipe is then as follows [32]. *i)* Initially, there is a small, fully connected, core of m_0 nodes. Assign to each of these m_0 nodes a random affinity a_i taken from a probability distribution. In this work, we have used for simplicity a uniform distribution between $(0, 1)$. *ii)* At each time step, a new node j with a random affinity a_j is introduced and m links are established with nodes already present in the network following the rule

$$\Pi(k_i) = \frac{k_i}{\sum_{s \in \Gamma} k_s}, \quad (1)$$

where the set Γ contains all nodes that verify the condition $a_i - \mu \leq a_j \leq a_i + \mu$, being $\mu \in (0, 1)$ a parameter that controls the affinity tolerance of the nodes. Finally, *iii)* repeat step (ii) t times such that the final size of the network be $N = m_0 + t$.

In the above model, when μ is close enough to 1, the BA model is recovered. When it is decreased from 1, the values of some magnitudes such as the clustering coefficient ($\langle c \rangle$) and the average path length ($\langle L \rangle$) grows with respect to the BA limit [32]. In Fig. 1 we have represented how these properties vary as a function of the parameter μ . Note that the larger variations correspond to the clustering coefficient (a factor greater than 4 as compared to a factor close to 2 for $\langle L \rangle$) and that it is the first property that deviates from the BA limit. This tendency holds up to very small values of μ , where $\langle L \rangle$ raises at a higher rate than $\langle c \rangle$ (not shown in Fig. 1). More important for our purposes is the region of $0.4 \leq \mu \leq 1$. For these values of μ one observes that $\langle L \rangle$ remains constant while $\langle c \rangle$ starts to grow as soon as it moves away from the BA limit ($\mu = 1$). This allows to decouple the effects of both magnitudes on what we are going to study. As we shall latter see, the structural clustering plays a major role in the synchronization of Kuramoto oscillators, as does in other dynamical processes [33].

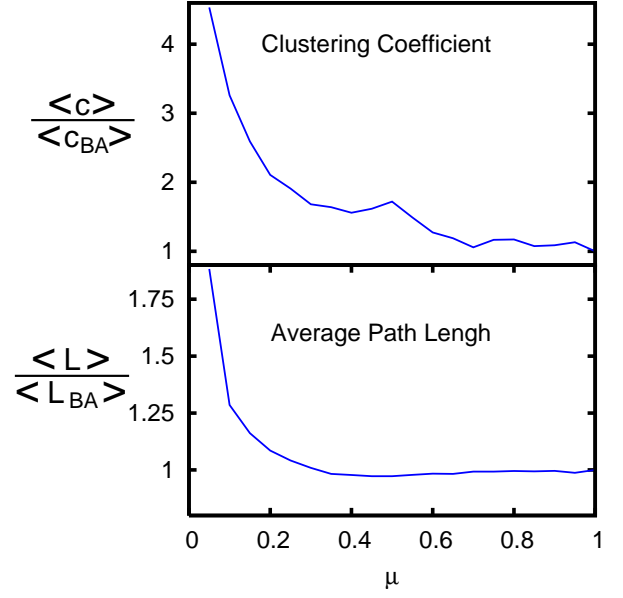


FIG. 1: (color online) Top: Values of the clustering coefficient relatives to those of the BA model against the parameter μ . Bottom: The average cluster length for the network generated relatives to the BA value as a function of μ . All the networks are made up of $N = 1000$ and have an average degree $\langle k \rangle = 6$.

The dynamic ingredient of the model is given by the collective behavior that arises when the nodes are considered to be phase oscillators that follow the Kuramoto model. In this formalism, the population of N interconnected units are coupled phase oscillators where the phase of the i -th unit, denoted by $\theta_i(t)$, evolves in time according to

$$\frac{d\theta_i}{dt} = \omega_i + \sum_j \Lambda_{ij} A_{ij} \sin(\theta_j - \theta_i) \quad i = 1, \dots, N \quad (2)$$

where ω_i stands for its natural frequency, $\Lambda_{ij} = \lambda$ [34] is the coupling strength between units and A_{ij} is the connectivity matrix ($A_{ij} = 1$ if i is linked to j and 0 otherwise). Note that in the original Kuramoto model mean-field interactions were assumed which leads to $\Lambda_{ij} = \mathcal{K}/N \forall i, j$, for the all-to-all architecture. On the other hand, the model can be solved in terms of an order parameter r that measures the extent of synchronization in a system of N oscillators as:

$$r e^{i\Psi} = \frac{1}{N} \sum_{j=1}^N e^{i\theta_j} \quad (3)$$

where Ψ represents an average phase of the system. The parameter r takes values $0 \leq r \leq 1$, being $r = 0$ the value of the incoherent solution and $r = 1$ the value for total synchronization.

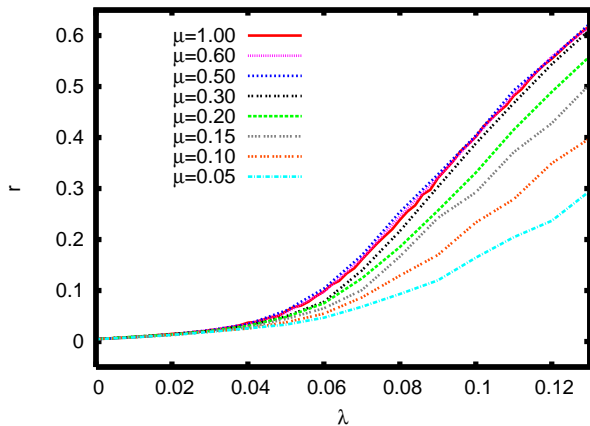


FIG. 2: (color online) Order parameter r as a function of λ for different values of μ as indicated. The network parameters are those of Fig. 1.

RESULTS

In order to inspect how the dynamics of the N oscillators depends on the underlying topology, we have performed extensive numerical simulations of the model. Starting from $\lambda = 0$, we increase at small intervals its value. The natural frequencies and the initial values of θ_i are randomly drawn from a uniform distribution in the interval $(-1/2, 1/2)$ and $(-\pi, \pi)$, respectively. Then, we integrate the equations of motion Eq. (2) using a 4th order Runge-Kutta method over a sufficiently large period of time to ensure that the system reaches the stationary state, where the order parameter r is computed. The procedure is repeated gradually increasing λ .

The results for r are shown in Fig. 2 against the control parameter λ for several networks characterized by different μ . For all values of μ , when the coupling is increased from small values, the incoherent solution prevails and macroscopic synchronization is not attained. This behavior persists until a certain critical value $\lambda_c(\mu)$ is crossed. At this point some elements lock their relative phase and synchronized nodes form. This constitutes the onset of synchronization. Beyond this value, the population of oscillators splits into a partially synchronized state contributing to r and a group of nodes whose natural frequencies are too spread as to be part of the coherent pack. Finally, after further increasing the value of λ , more and more nodes get entrained around the mean phase and the system settles in a completely synchronized state where $r \approx 1$ (not shown).

A comparison between the results for different values of μ (and thus different $\langle c \rangle$ and $\langle L \rangle$ values) indicate several interesting features of the synchronization process. First, it is remarkably that when the clustering coefficient increases, the system reaches *complete synchronization* at higher values of the coupling. This result agrees with the results reported in [27], where a different network model able to generate topologies with a tunable clustering coefficient was implemented.

At this point, one may ask whether the effects are only due to the influence of $\langle c \rangle$ or to the increase of the average path length [35] (note that the model implemented in [27] does not explore this possibility). Unfortunately, the two factors are generally linked together so they can not be considered separately. However, as stated previously, a closer look at Fig. 1 reveals that there is a region of the parameter μ where the clustering coefficient grows while the average shortest path length remains almost constant. This corresponds to the interval $0.4 \leq \mu \leq 1.0$ approximately. Going back to Fig. 2, the behavior of r in this interval of μ reveals that synchronization is almost unaffected. In fact, the $r(\mu)$ curves lie slightly above that corresponding to the BA limit. Therefore, though the above comparison is not conclusive, it seems that the delayed transition to complete synchronization is mainly due to the effect of the increase in $\langle L \rangle$ at smaller values of μ rather than to the increase in $\langle c \rangle$. This conclusion is further supported by a direct comparison of the results in Fig. 2 with those reported in [27], where the authors explored a region with higher values of $\langle c \rangle$ (up to 0.7) and the profile of $r(\lambda)$ is almost the same as ours.

The second region of interest is the onset of synchronization. From Fig. 2, it is difficult to elucidate how the critical point for the BA limit compares with those at values of $\mu < 1$. At first glance, it seems that $\lambda_c(\mu)$ shifts rightward as the parameter μ is decreased below 1. However, a more detailed analysis shows that it is indeed the contrary. To this end, we have performed a finite size scaling analysis that allows to determine the critical points $\lambda_c(\mu)$. We assume a scaling relation of the form

$$r = N^{-\alpha} f(N^\beta(\lambda - \lambda_c)), \quad (4)$$

where $f(x)$ is a universal scaling function bounded as $x \rightarrow \pm\infty$ and α and β are critical exponents to be determined. The estimation of λ_c can then be done by plotting $N^\alpha r$ as a function of λ and tuning α for several system sizes N until the curves cross at a single point, the critical one.

The results of the FSS analysis are shown in Fig. 3 for different values of μ (from top to bottom and from left to right $\mu = 0.05, 0.15, 0.50, 0.60$). The insets show a blow-up around the critical points $\lambda_c(\mu)$. Although the differences in the critical points at different values of μ are small, they are certainly distinguishable. In fact, the higher the value of μ , the higher the critical point. That is, when the clustering coefficient and the average path length grow with respect to the BA network, the onset of synchronization is anticipated. Moreover, taking into account that the increase in $\langle L \rangle$ is likely to inhibit synchronization, one may hypothesize that the effects of the clustering coefficient prevail in this region of the parameter λ . To check this hypothesis, we have also included in Fig. 3 the analysis performed for $\mu = 0.50$ and $\mu = 0.60$. As pointed out before, for these values, the differences can only arise from the variations of the clustering coefficient as the average path length remains constant in this region of the parameter μ . The critical points, although very close to each other, are clearly different. Therefore, the main contribution

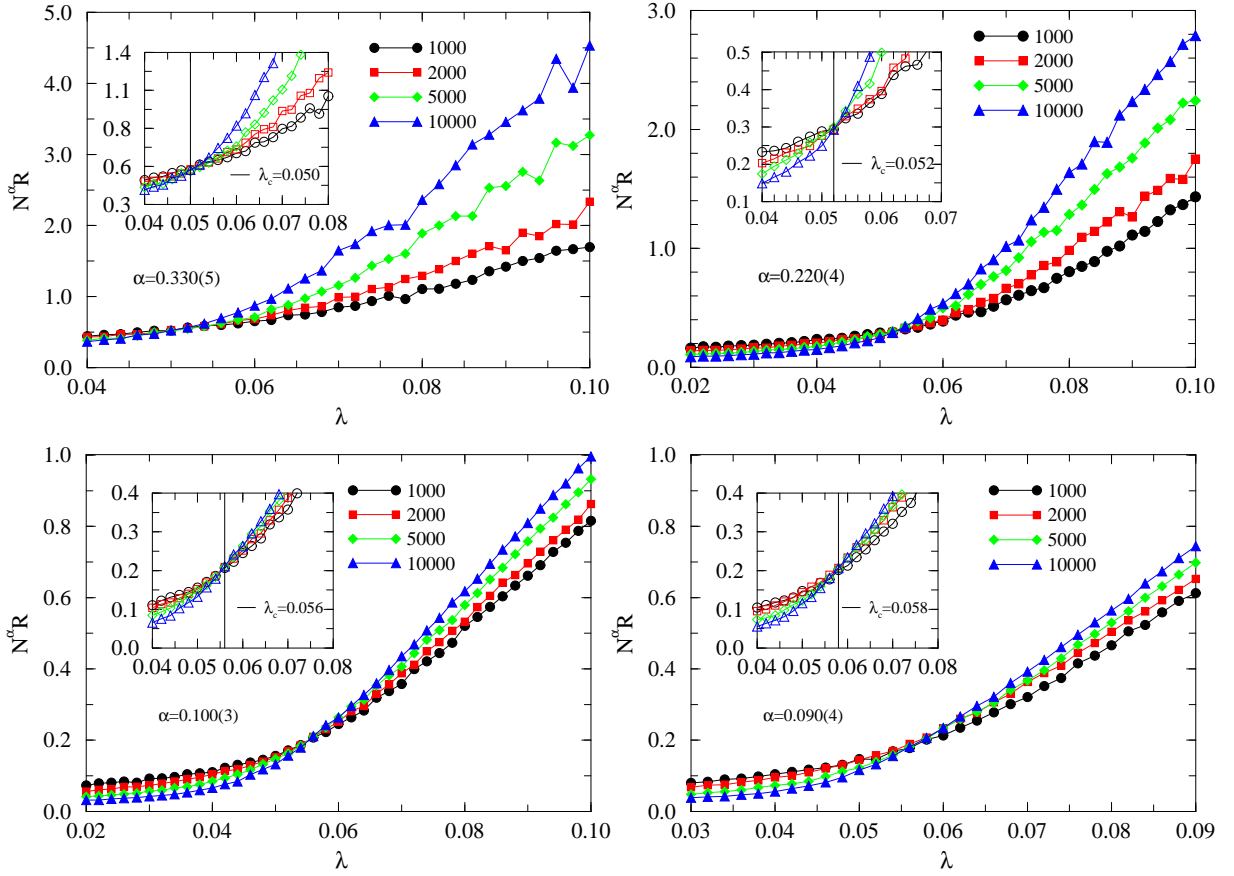


FIG. 3: (color online) Finite size scaling analysis for several values of μ . From top to bottom and from left to right the values of μ are: 0.05, 0.15, 0.50 and 0.60. In each panel, it is represented the rescaled order parameter against the control parameter λ . The insets are a zoom to the regions around the critical points $\lambda_c(\mu)$. The data are averaged over at least 100 realizations for each value of λ . The sizes of the networks, the critical points $\lambda_c(\mu)$ at which the onset of synchronization takes place, as well as the values of the critical exponents α are those indicated in the plots. See the main text for more details.

to the onset of synchronization at low values of λ comes from the raising of the clustering coefficient.

DISCUSSIONS AND CONCLUSIONS

Rounding off, our results point to a nontrivial dependence between the clustering coefficient and the average path length, and the synchronization patterns of phase oscillators. Separately, the onset of synchronization seems to be mainly determined by $\langle c \rangle$, promoting synchronization at low values of the coupling strength with respect to networks not showing high levels of structural clustering. On the other hand, when the coupling is increased beyond the critical point, the effect of $\langle L \rangle$ dominates and the phase diagram is smoothed out (a sort of stretching), delaying the appearance of the fully synchronized state. These results confirm and complement those anticipated in [27] and show that general statements about synchronizability using the MSF are misleading. Whether or not a system is more or less synchronizable than others show-

ing distinct structural properties is relative to the region of the phase diagram in which the system operates [29, 30].

In summary, we have shown that synchronizability of complex networks is dependent on the effective coupling λ among oscillators, and on the properties of the underlying network. For small values of λ , the incoherent solution $r = 0$ first destabilizes as the clustering coefficient is higher, while the coherent solution $r = 1$ is promoted when both the structural clustering and the average path length are small. Finally, we point out that our results are also consistent if a different local order parameter is considered [30]. Moreover, though these results have been obtained for phase oscillators, we think that they should hold for other nonlinear dynamical systems as well. It would be interesting to check this later hypothesis in future works.

We thank A. Arenas for helpful comments and discussions on the subject. J.G.G. and Y.M. are supported by MEC through a FPU grant and the Ramón y Cajal Program, respectively. This work has been partially supported by the Spanish DGICYT Projects FIS2004-05073-C04-01 and FIS2005-

00337.

-
- [1] A. T. Winfree, *The geometry of biological time* (Springer-Verlag, New York, 1990).
- [2] S. H. Strogatz, *Sync: The Emerging Science of Spontaneous Order* (New York: Hyperion, 2003).
- [3] S. C. Manrubia, A. S. Mikhailov, and D. H. Zanette, *Emergence of Dynamical Order. Synchronization Phenomena in Complex Systems* (World Scientific, Singapore, 2004).
- [4] Y. Kuramoto, *Chemical oscillations, waves, and turbulence* (Springer-Verlag, New York, 1984).
- [5] J. A. Acebrón, L. L. Bonilla, C. J. Pérez Vicente, F. Ritort, and R. Spigler, *Rev. Mod. Phys.* **77**, 137 (2005).
- [6] M. E. J. Newman, *Proc. Natl. Acad. Sci. U.S.A.* **98**, 404 (2001).
- [7] H. Jeong, S. P. Mason, A.-L. Barabási, and Z. N. Oltvai, *Nature (London)* **411**, 41 (2001).
- [8] R. V. Solé, and J. M. Montoya, *Proc. R. Soc. London B* **268**, 2039 (2001).
- [9] M. Faloutsos, P. Faloutsos, and C. Faloutsos, *Proceedings of the ACM, SIGCOMM* [Comput. Commun. Rev. **29**, 251 (1999)]
- [10] F. Wang, Y. Moreno, and Y. Sun, *Physical Review E* **73**, 036123 (2006).
- [11] S. N. Dorogovtsev and J. F. F. Mendes, *Evolution of Networks. From Biological Nets to the Internet and the WWW*, Oxford University Press, Oxford, U.K., (2003).
- [12] *Handbook of Graphs and Networks*, Edited by S. Bornholdt and H. G. Schuster, Wiley-VCH, Germany, 2003.
- [13] S. Boccaletti, V. Latora, Y. Moreno, M. Chavez, and D.-U. Hwang, *Complex networks: Structure and dynamics*, *Phys. Rep.* **424**, 175 (2006).
- [14] R. Pastor-Satorras and A. Vespignani. *Phys. Rev. Lett.* **86**, 3200 (2001).
- [15] R. Pastor-Satorras and A. Vespignani. *Phys. Rev.* **E63**, 066117 (2001).
- [16] Y. Moreno, R. Pastor-Satorras, and A. Vespignani, *Eur. Phys. J.* **B26** 521 (2002).
- [17] R. Cohen, K. Erez, D. ben Avraham, and S. Havlin, *Phys. Rev. Lett.* **85**, 4626 (2000).
- [18] L. M. Pecora and T. L. Carroll, *Phys. Rev. Lett.* **80**, 2109 (1998).
- [19] M. Barahona and L. M. Pecora, *Phys. Rev. Lett.* **89**, 054101 (2002).
- [20] T. Nishikawa, A.E. Motter, Y.-C. Lai, and F.C. Hoppensteadt, *Phys. Rev. Lett.* **91**, 014101 (2003).
- [21] A.E. Motter, C. Zhou, and J. Kurths, *Phys. Rev. E* **71**, 016116 (2005).
- [22] L. Donetti, P. I. Hurtado, and M. A. Muñoz, *Phys. Rev. Lett.* **95**, 188701 (2005).
- [23] C. Zhou, A. E. Motter, J. Kurths, *Phys. Rev. Lett.* **96**, 034101 (2006).
- [24] M. Chavez, D.-U. Hwang, A. Amann, H. G. E. Hentschel, S. Boccaletti, *Phys. Rev. Lett.* **94**, 218701 (2005)
- [25] Y. Moreno and A. F. Pacheco, *Europhys. Lett.* **68**, 603, (2004).
- [26] E. Oh, K. Rho, H. Hong, and B. Kahng, *Phys. Rev. E* **72**, 047101 (2005).
- [27] P. N. McGraw and M. Menzinger, *Phys. Rev. E* **72**, 015101(R) (2005).
- [28] A. Arenas, A. Díaz-Guilera and C.J. Pérez-Vicente, *Phys. Rev. Lett.* **96**, 114102, (2006).
- [29] J. Gómez-Gardeñes, Y. Moreno and A. Arenas, unpublished.
- [30] J. Gómez-Gardeñes, Y. Moreno and A. Arenas, in preparation.
- [31] A.-L. Barabási, and R. Albert, *Science* **286**, 509 (1999).
- [32] J. Gómez-Gardeñes, and Y. Moreno, *Physical Review E* **69**, 037103 (2004).
- [33] P. Echenique, J. Gómez-Gardeñes, and Y. Moreno, *Physical Review E* **70**, 056105 (2004).
- [34] We refer to Refs [29, 30] for a discussion on the proper choice of the coupling strength describing the interaction between the oscillators.
- [35] Note that although the main differences in the network model are observed for $\langle c \rangle$ and $\langle L \rangle$, other properties may slightly vary as well.